Downloaded via KING ABDULLAH UNIV SCI TECHLGY on December 19, 2018 at 05:28:26 (UTC).
See https://pubs.acs.org/sharingguidelines for options on how to legitimately share published articles.

I&EC research
Industrial & Engineering Chemistry Research

Article

Cite This: *Ind. Eng. Chem. Res.* 2018, 57, 17003−17012

pubs.acs.org/IECR

Evaluation of Carbon Nanotubes and Quartz Sand for the Removal of Formaldehyde−(2,4-Dinitrophenylhydrazine) from Aqueous Solutions

Maria P. Georgopoulou and Constantinos V. Chrysikopoulos*

School of Environmental Engineering, Technical University of Crete, Chania, 73100, Greece

ABSTRACT: The assessment of the potential impact of engineered carbon nanotubes on the removal of synthetic chemical contaminants (e.g., pesticides, pharmaceuticals, and chemical reaction products) from aqueous solutions has become an increasingly important aspect of environmental research. This study has focused on the interaction of the reaction product of formaldehyde (FA) with 2,4-dinitrophenylhydrazine (2,4-DNPH) with multiwalled carbon nanotubes (MWCNTs) and quartz sand under static and dynamic conditions. Several batch adsorption experiments were conducted in test tubes, under controlled conditions and at laboratory room temperature (23 °C). The experimental results suggested that FA−(2,4-DNPH) has a low affinity for quartz sand but an enhanced potential for adsorption onto small quantities of MWCNTs. FA−(2,4-DNPH) adsorption onto quartz sand and MWCNTs was more pronounced under dynamic than static conditions, probably due to agitation improved mixing of the absorbent within the solution. The collected adsorption data were adequately described by a pseudo-second-order kinetic model and intraparticle diffusion model. On the basis of root-mean-square error (RMSE) values, better fitting of experimental data was achieved with the Weber-Morris intraparticle diffusion model. Our findings suggested that a rapid surface chemisorption of FA−(2,4-DNPH) onto available adsorption sites of sand and MWCNTs, followed by a slower intra-aggregate diffusion of FA−(2,4-DNPH) onto interstitial spaces of entangled MWCNTs, occurred. The observed FA−(2,4-DNPH) removal by combined MWCNTs and quartz sand was 78.1%. Thus, MWCNTs could be promising adsorbent materials for removal of complicated organic compounds from aqueous solutions and for groundwater remediation.

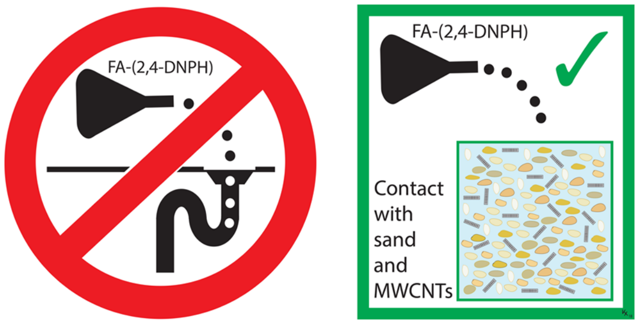

1. INTRODUCTION

Formaldehyde (FA), with molecular formula CH_2O, is ranked among the most commonly manufactured and among the most frequently occurring organic chemical compounds in the environment.[1,2] The use of FA in many industrial fields, such as in the petrochemical industry, furniture industry, aquaculture industry, tannery industry, adhesive manufacturing, glue and paper manufacturing, cosmetic industry, and textile and wood processing,[3−6] as well as in clinical anatomy laboratories as a preservative for cadavers and organs,[7] enhances its potential for environmental release through mixed and industrial liquid effluents.[2,8−10] Note that conventional biotreatment of liquid wastes containing high concentrations of FA (800−1500 mg/L) is practically impossible because FA inhibits the action of microorganisms or may even cause their death.[7,8,11] In addition, its high water solubility and low partition coefficient ($\log K_{ow} = 0.35$) suggest that the potential for adsorption of FA onto suspended sediments in aqueous environmental systems is low. Thus, dissolved FA present in effluents from sewage treatment plants or in other aqueous solutions is expected to infiltrate into the soil and, subsequently, may contaminate surface and ground waters.

The maximum acceptable FA concentration threshold that can be assimilated from an aquatic environment without disturbing its ecosystem balance is 1.61 mg/L.[7,12] FA has been classified as a human carcinogen by inhalation, but not via the oral route (Carcinogenity category 1B), and as a probable mutagenicity-involved substance (Mutagenicity category 2).[13,14] However, FA is not included on the guideline lists of the International Conference on Harmonisation (ICH), and thus, its threshold value has not been established. On the basis of the health guidelines and the criteria for water quality proposed by the US Environmental Protection Agency (EPA), the FA maximum daily dose reference is approximately 0.2 mg/kg, while a value of 0.35 mg/L (or one-day exposure at 10 mg/L) in drinking water is considered to be acceptable.[15]

Given that numerous FA-related negative health effects exist,[16] it is of vital importance to quantify FA in water samples. Unfortunately, FA determination and quantification in aqueous solutions is not a trivial task. Analysis of FA using

Received: August 19, 2018
Revised: October 23, 2018
Accepted: November 20, 2018
Published: November 20, 2018

ACS Publications © 2018 American Chemical Society

DOI: 10.1021/acs.iecr.8b03996

mass spectrometry or gas chromatography is a difficult task because FA molecules are not easily ionizable.[17] Among the available analytical approaches, which have been developed for the detection of FA,[10,18−21] high-performance liquid chromatography (HPLC) is considered to be the most convenient method.[17,22−24]

The HPLC-based analytical determination of FA is achieved through the derivatization reaction of FA with 2,4-dinitrophenylhydrazine (DNPH) reagent, with molecular formula $C_6H_6N_4O_4$, to form methanol 2,4-dinitrophenylhydrazone, a yellow derivative, which can be observed spectrophotometrically.[22−27] The reaction equation is $CH_2O + C_6H_6N_4O_4 \rightarrow C_7H_6N_4O_4 + H_2O$. An unfortunate but inevitable consequence of the chemical derivatization process of FA is the production of hazardous HPLC wastes in liquid form, consisting of the derivatives mixed with flammable, toxic, and volatile organic solvents such as acetonitrile, hexane, methanol, methylene chloride, ethyl acetate, and trifluoroacetic acid. Because HPLC is a widely applied analytical separation and quantification technique, production of large quantities *o*f hazardous wastes is expected. Disposal of these wastes is often highly regulated.[28,29] However, our understanding of the environmental behavior of these potentially harmful chemicals and their effects on human health remains limited. Although many of the currently available laboratory HPLC waste collection and management techniques are designed to protect against spills and leaks, they do not provide a completely safe work environment.[30]

Among the various physicochemical techniques available for the removal of organic contaminants from aqueous solutions (e.g., catalytic and photocatalytic degradation,[31−37] ion exchange, reverse osmosis, and stripping), adsorption remains the predominant process due to its effectiveness, simplicity in application, and low cost.[38] The most frequently used adsorbents in filtration systems are quartz sand, clay minerals (e.g., zeolite, montmorillonite, and kaolinite), molecular sieves, resins, silica gels, and bioadsorbents[39] as well as carbon-based materials like activated carbon (AC).[40] However, the allotropic nanoscale carbon materials (e.g., graphene, single- and multiwalled carbon nanotubes, and fullerenes) are currently receiving substantial attention.[41−43]

Among the available synthetic nanomaterials, multiwalled carbon nanotubes (MWCNTs), consisting of multiple superimposed layers of graphene sheets rolled up into concentric hollow cylinders, have attracted special industrial and commercial interest.[44,45] Due to their structure and dimensionality, MWCNTs possess enhanced physicochemical[46] and electrical[47−50] properties, thermal stability,[51] and mechanical strength.[52−55] Consequently, MWCNTs are often used in various fields, including reinforced composites, renewable energy technologies,[56] optoelectronics,[57−59] the food industry, and cosmetics, as well as in medical and biomedical applications.[60−63]

Due to their structural cavity, extremely small sizes, high specific surface area, and chemically inert surfaces, MWCNTs can strongly interact with organic pollutants.[64] The porous nature of MWCNTs enhances their adsorbent potential for the removal of a wide range of molecular organic pollutants from contaminated liquids. Note that MWCNTs are considered as very effective new carbon-based adsorbents in environmental pollution management[65] and wastewater treatment,[38,66] as well as in environmental protection and remediation.[67,68]

Many theoretical and experimental studies have focused on the interaction of CNTs with pollutants such as polycyclic aromatic hydrocarbons (PAHs),[69] dioxin,[70] fluoride,[71] nicotine and tar,[72] trihalomethanes,[73] tetracycline,[74] sulfonamide antibiotics,[75] and dyes,[42,76,77] highlighting the strong adsorption capacity and efficiency of MWCNTs.

Thus, new improved filtration techniques based on advanced nanomaterials like MWCNTs could be developed for both laboratory and field scale applications, in order for large volumes of produced hazardous organic wastes, like HPLC produced waste, to be managed and disposed of without significant health or environmental implications.

To our knowledge, the interaction of FA−(2,4-DNPH) solution with multiwalled carbon nanotubes has not been explored in any previous studies. In this work, kinetic batch experiments were conducted under static and dynamic conditions in order to study the adsorption behavior of FA−(2,4-DNPH) onto quartz sand, MWCNTs, and quartz sand mixed with carbon nanotubes. The effect of contact time and type of adsorbent was examined. The two types of adsorbent used were unmodified multiwalled carbon nanotubes (NTX1) and quartz sand. Quartz sand, consisting mainly of SiO_2 (96.2%), was employed in this study due to its wear resistance and stability of its chemical properties.

2. MATERIALS AND METHODS

2.1. Formaldehyde−DNPH Solution. A dense (1000 mg/L) FA stock solution was prepared by adding 124 μL of FA (37 wt %) solution to a 50 mL volumetric flask and diluting to volume with ultrapure water. All standard working solutions were prepared by diluting the stock solution with ultrapure water to the appropriate concentration. The stock solutions were stored in the dark at 4 °C until use.[26] A DNPH solution (0.1 mg/L) was prepared by dissolving 5.15 mg of 2,4-dinitrophenylhydrazine reagent (97%) into a 50 mL volumetric flask containing approximately 10 mL of acetonitrile (ACN). After sonication for 3 min, in order to achieve proper dissolution of the reagent, the solution was diluted to volume with ACN. The reaction of FA with DNPH was facilitated in an acidic environment.[24] Thus, a 5 N phosphoric acid solution was prepared by adding 195 μL of H_3PO_4 (85%) with a piston pipet into a 50 mL volumetric flask and diluted to volume with ultrapure water. The standard reagent of the 2,4-dinitrophenylhydrazone derivative of FA used for quantification was synthesized according to a previously developed method.[17] To a suitable vial, 1 mL of 0.1 mg/L FA standard solution, 20 μL of 5 N H_3PO_4, and 200 μL of 2,4-DNPH solution were added. The resulted mixture was stirred on a shaker for at least 30 min. All reagents used in this study were purchased from Sigma-Aldrich, St. Louis, USA.

All analytical concentration determinations were performed on an HPLC system (Shimadzu Corporation, Kyoto, Japan), equipped with a diode array detector (DAD) and two solvent delivery pumps. An Ultrasphere 5 μm ODS column (250 × 4.6 mm, Hichrom) was used to separate the target analytes at 30 °C. The mobile phase was acetonitrile and water in the ratio of 80:20 v/v, at a flow rate of 1.0 mL/min. The injection volume was 20 μL, and detection wavelength was set at 360 nm. The total analysis time was 4 min.

To a suitable vial, 1 mL of 10 mg/L FA solution, 20 μL of 5 N H_3PO_4, and 20 mL of 2,4-DNPH solution were added. The mixture was stirred for 30 min. The concentration of the standard FA−(2,4-DNPH) solution was 10 mg/L, from which

DOI: 10.1021/acs.iecr.8b03996
Ind. Eng. Chem. Res. 2018, 57, 17003−17012

various calibration FA−(2,4-DNPH) solutions of lower concentration (0.1, 0.5, 1, 2, and 5 mg/L) were prepared by dilution. Then, 20 μL of each calibration solution was injected in HPLC in duplicates, and a calibration curve was obtained by liner regression of the peak area of FA−(2,4-DNPH) versus concentration. The regression equation obtained was

$$C_{\text{FA}-(2,4\text{-DNPH})} = 2.231 \times 10^{-6}\,(\text{area}) - 0.0526 \tag{1}$$

where $C_{\text{FA}-(2,4\text{-DNPH})}$ [mg/L] is the FA−(2,4-DNPH) concentration and area is the peak area of FA−(2,4-DNPH). The correlation coefficient was 0.999.

2.2. Quartz Sand. Quartz sand (Filcom Filterzand & Grid, Netherlands) was employed in this study because this mineral is widely used in water filtration techniques. The main chemical component of the examined sand was SiO_2 (96.2%). The grain diameter of the quartz sand used ranged from 0.425 to 0.600 mm (sieve no. 30/40). The uniformity coefficient (C_u), the specific gravity, and the bulk density of the quartz sand were 1.21, 2.6 g/cm^3, and 1.6 g/cm^3, respectively. The specific surface area (SSA) of the quartz sand used was estimated to be 73.2 cm^2/g. On the basis of the Walkley-Black method,[78] the content of the total organic carbon (TOC) of the sand was estimated to be equal to 0.1 ± 0.1%. The quartz sand was thoroughly cleaned with 0.1 M nitric acid (HNO_3, 70%) for 3 h to remove surface impurities (e.g., metal hydroxides and organic coatings), rinsed with distilled deionized water (ddH_2O), then soaked in 0.1 M NaOH for 3 h, and rinsed with ddH_2O again.[79] Subsequently, the sand was sterilized and dried at 80 °C overnight and then stored in screw cap beakers until use in batch experiments.

2.3. Multiwalled Carbon Nanotubes (MWCNTs). High carbon purity (>97%) pristine MWCNTs (NTX1), produced by catalytical chemical vapor deposition, with outer diameter in the range of 15−35 nm and length of ≥10 mm, were purchased from NanothinX S.A. (Patras, Greece). According to the manufacturer, the amorphous carbon content was less than 1%, metal impurities content was approximately 3%, and the bulk density of the product was 0.167 g/cm^3. On the basis of the BET (Brunauer, Emmett and Teller) method, the specific surface area (SSA) of MWCNTs was estimated to be 205 m^2/g.[80] Moreover, the surface charge of the suspended MWCNTs was measured with a zetasizer (Nano ZS90, Malvern Instruments, Southborough, MA) as −13.5 mV ± 3.16 mV, indicating a strong aggregation tendency. During the batch adsorption experiments, the multiwalled carbon nanotubes were used in powder, pristine form as opposed to suspended form.

2.4. Batch Experiments. Static and dynamic batch experiments were performed in 20 mL Pyrex glass screw cap tubes (Fisher Scientific), under controlled conditions at room temperature using a FA−(2,4-DNPH) concentration of 9 mg/L. Prior to each experiment, the glass tubes were washed with detergent, rinsed thoroughly in ddH_2O, autoclave sterilized, and oven-dried at 80 °C overnight. Three different groups of adsorption experiments were analyzed. For the first group, the glass tubes contained 14 mL of FA−(2,4-DNPH) and 14 g of quartz sand. For the second group, the glass tubes contained 14 mL of FA−(2,4-DNPH), 14 g of quartz sand, and 20 mg of NTX1. For the third group, the glass tubes contained 20 mL of FA−(2,4-DNPH) and 20 mg of NTX1. For each adsorption experiment, 16 glass tubes were employed. All glass tubes were filled to the top. For the dynamic batch experiments, the glass tubes were attached onto a rotator (Selecta, Agitador orbit), operated at 12 rpm, in order to allow the sand and MWCNTs to better mix within the FA−(2,4-DNPH) solution. Total duration of each experiment was 20 days (d). Supernatant liquid samples of 2 mL were collected at preselected time intervals (1 h, 2 h, 3 h, 6 h, 12 h, 24 h, 2 d, 3 d, 5 d, 7 d, 10 d, 12 d, 14 d, 16 d, 18 d, and 20 d) and centrifuged at 4000 rpm or 2500g, for 15 min (Rotofix 32A, Hettich), to remove soil particles and nanoparticles. Approximately 1 mL of the supernatant was injected into the HPLC for analysis at 360 nm.

3. THEORETICAL CONSIDERATIONS

Although numerous adsorption kinetics models are available (e.g., first-order, second-order, pseudo-first-order, pseudo-second-order, and intraparticle diffusion), preliminary analysis of the experimental data collected in this study suggested that the pseudo-second-order and intraparticle diffusion models were more applicable. Note that the intraparticle diffusion model is used in this study to characterize intra-aggregate diffusion. The pseudo-second-order model is expressed as:[81,82]

$$\frac{dC_t^*}{dt} = k_{p2}(C_{eq}^* - C_t^*)^2 \Rightarrow C_t^* = \frac{(C_{eq}^*)^2 k_{p2} t}{1 + C_{eq}^* k_{p2} t} \tag{2}$$

where C_{eq}^* [mg/g] is the FA−(2,4-DNPH) concentration sorbed onto the solid phase at equilibrium; C_t^*[mg/g] is the FA−(2,4-DNPH) concentration sorbed onto the solid phase at time t; k_{p2} [g/mg·d] is the rate constant of the pseudo-second-order adsorption; t [d] is time. Typically, the applicability of this model indicates that the prevailing step of the adsorption mechanism (i.e., rate limiting step) is chemical sorption between the adsorbed substance and the adsorbent. During chemical interaction, it is possible that electron exchange or valent forces take place between the adsorbed substance and the adsorbent.[81] However, it should be noted that the pseudo-second-order model is classified as an adsorption-reaction model, derived from the kinetics of chemical reactions, which examines the total adsorption process without consideration of other possible intermediate adsorption steps (e.g., diffusion through film, intraparticle diffusion, etc.).[81] The intraparticle diffusion model examined in this study is known as the Weber-Morris model and is expressed as follows:[83−85]

$$C_t^* = k_{\text{intrap}} t^{1/2} + C_{\text{inters}}^* \tag{3}$$

where k_{intrap} [mg/g·d$^{1/2}$] is the intraparticle diffusion rate constant and C_{inters}^* [mg/g] is the intraparticle diffusion constant (y-intercept), which is proportional to the boundary layer thickness.[86] According to Weber-Morris model, the relationship between $C_t^*$and $t^{1/2}$ indicates the existence of one or more regulatory steps in the adsorption process. This model is classified as the adsorption−diffusion model and assumes that the adsorption mechanism consists of three main stages: diffusion through the interface, diffusion through pores, and intraparticle diffusion, with the slowest stage controlling the process.[81] Generally, in batch processes, where the resistance of the boundary layer is not restrictive, the regulatory steps are usually diffusion through pores and intraparticle diffusion, while in continuous processes the rate-limiting step is more likely to be interface diffusion (i.e., film diffusion).[87] When the intraparticle diffusion is the sole rate-limiting step, the regression between C_t^* and $t^{1/2}$ is linear with slope k_{intrap},

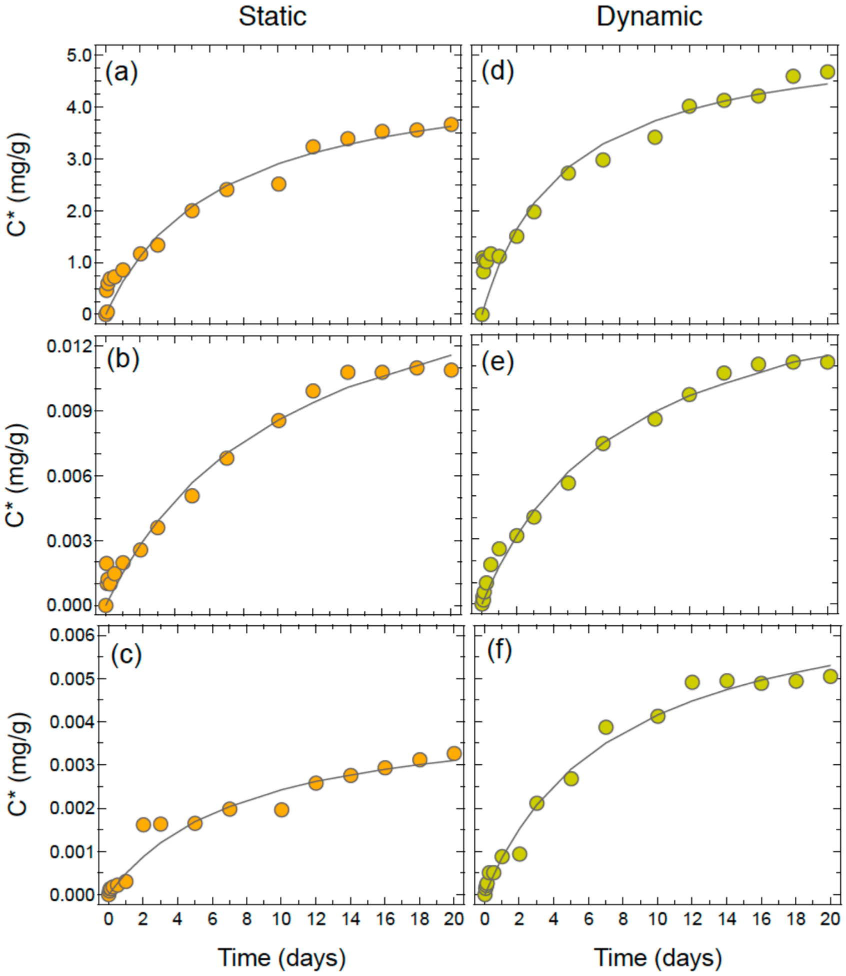

Figure 1. Adsorption of FA−(2,4-DNPH) onto (a, d) NTX1, (b, e) quartz sand mixed with NTX1, and (c, f), quartz sand, under (a−c) static and (d−f) dynamic conditions for a time period of 20 days based on the pseudo-second-order kinetic model. Here, C_0 = 9 mg/L at 23 °C.

passing through the origin. The formation of more lines of different slope (i.e., linear parts) suggests the existence of different adsorption rates and that intraparticle diffusion may not be the only controlling adsorption mechanism. In certain cases, the total adsorption process can be controlled by either a single step (e.g., film or external diffusion, pore diffusion, surface diffusion, and adsorption to the surface of pores) or a combination of more than one step.[81,87] Note that a positive y-axis intercept indicates rapid adsorption rate in the early stages of the adsorption process, while a negative y-axis intercept reflects the impact of the existence of resistance during film diffusion.[87,88]

The concentration of FA sorbed onto the sorbent at a particular sampling time was calculated by the following equation:

$$C_t^* = \frac{(C_0 - C_t)}{W} V \tag{4}$$

where C_0 [mg/L] is the initial FA−(2,4-DNPH) concentration in the aqueous phase; C_t [mg/L] is the FA−(2,4-DNPH) concentration in the aqueous phase at time t; V [L] is the total volume of FA−(2,4-DNPH) solution added per vial; W [g] is the adsorbent mass added in the glass tube. If more than one adsorbent was used simultaneously, the above expression provides the total mass adsorbed onto all of the adsorbents used, as opposed to the mass adsorbed onto each adsorbent separately. Furthermore, the FA−(2,4-DNPH) removal was calculated by the following equation:

$$\text{removal (\%)} = \frac{(C_0 - C_t)}{C_0} \times 100 \tag{5}$$

The root-mean-square error (RMSE) was used for adsorption model discrimination. The RMSE represents the sample standard deviation of the differences between values predicted by a model and experimentally observed values (i.e., the square root of the variance of the residuals or equivalently the spread of the points about the fitted regression line), and it is evaluated by the following equation:

$$\text{RMSE} = \sqrt{\frac{\sum_{i=1}^{n} (X_{\text{exp},i} - X_{\text{model},i})^2}{n}} \tag{6}$$

where $X_{\text{exp},i}$ and $X_{\text{model},i}$ are the experimental and modeled values at time i, respectively. RMSE has the same units as the response variable. Lower RMSE values indicate better fit. Also, RMSE is sensitive to outliers (i.e., observations that take on extreme values compared to the majority of the data).[89,90]

4. EXPERIMENTAL RESULTS AND DISCUSSION

The static and dynamic batch experimental data were presented in Figure 1 together with the pseudo-second-order kinetic model best fitted curves constructed with the ColloidFit

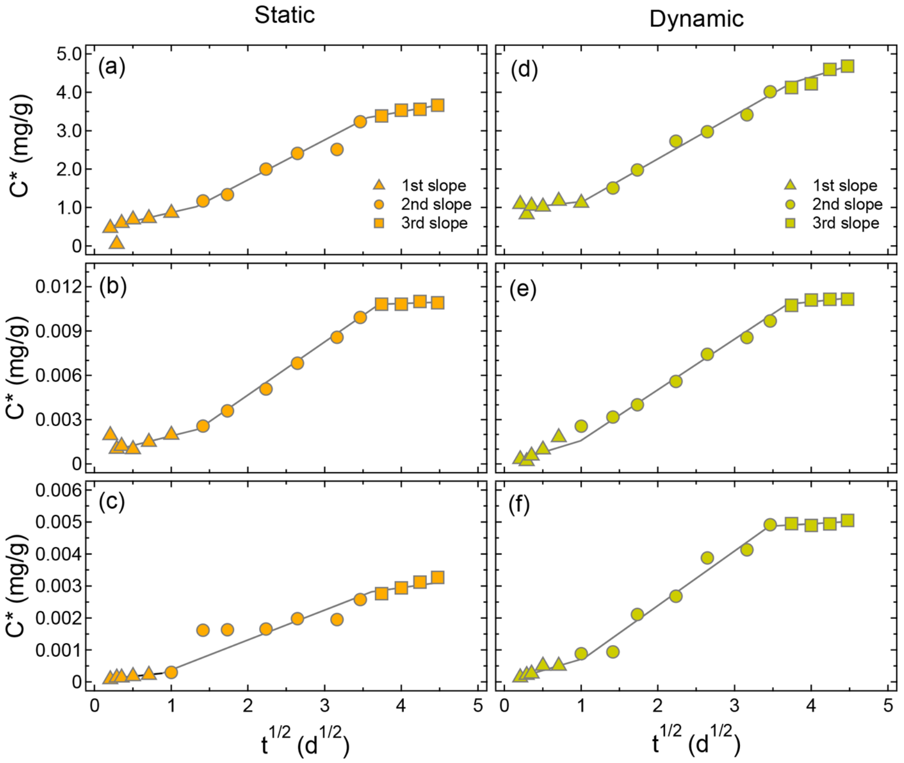

Figure 2. Adsorption of FA−(2,4-DNPH) onto (a, d) NTX1, (b, e) quartz sand mixed with NTX1, and (c, f), quartz sand, under (a−c) static and (d−f) dynamic conditions for a time period of 20 days based on the Weber-Morris intraparticle diffusion kinetic model. Here, C_0 = 9 mg/L at 23 °C.

Table 1. Fitted Parameter Values and Calculated RMSE Values for the FA−(2,4-DNPH) Kinetic Adsorption Experiments

	pseudo-second-order model			intraparticle diffusion model			
adsorbent	k_{p2} [g/mg·d]	C^*_{eq} [mg/g]	RMSE [mg/g]	linear part	k_{intrap} [mg/d$^{1/2}$·g]	C^*_{inters} [mg/g]	RMSE [mg/g]
			Static				
FA and NTX1	0.0317	4.8178	0.2673	1	0.4583	0.4137	0.1662
				2	1.0403	−0.3593	
				3	0.3532	2.0839	
FA and NTX1 and sand	5.3760	0.0177	0.00072	1	0.00130	0.0006	0.00032
				2	0.00359	−0.00252	
				3	0.00019	0.01009	
FA and sand	29.6658	0.0043	0.00026	1	0.00026	0.00005	0.00029
				2	0.00093	−0.00055	
				3	0.00033	0.00161	
			Dynamic				
FA and NTX1	0.0389	5.4973	0.4869	1	0.2211	0.9332	0.1072
				2	1.1363	−0.0034	
				3	0.5967	2.0154	
FA and NTX1 and sand	7.3758	0.0163	0.00042	1	0.00159	−0.000001	0.00035
				2	0.00343	−0.00182	
				3	0.00054	0.00881	
FA and sand	17.8761	0.0073	0.00025	1	0.00071	0.00001	0.00018
				2	0.00171	−0.00103	
				3	0.00014	0.00438	

software[91,92] and in Figure 2 together with the Weber-Morris intraparticle diffusion model best fitted curves constructed with Igor Pro (Wavemetrics, Lake Oswego, OR, USA). The fitted parameter values and the calculated RMSE values for both kinetic models were listed in Table 1. The removal of FA−(2,4-DNPH) was determined at each sampling interval using the eq 5, and the results were presented in Figure 3. Also, the normalized FA−(2,4-DNPH) concentration values at various times under dynamic and static conditions were presented in Figure 4. Furthermore, the removal of FA−(2,4-DNPH) after 20 days contact time and the removal differences between static and dynamic conditions were presented in Table 2.

A mixture of 14 g of quartz sand and 20 mg of multiwalled carbon nanotubes (NTX1) resulted in higher FA−(2,4-DNPH) removal than the removal obtained using the two adsorbents separately (see Figure 3). NTX1 exhibited greater

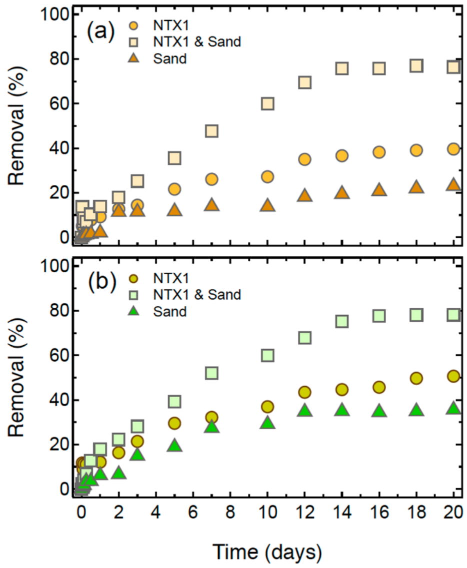

Figure 3. Removal of FA−(2,4-DNPH) under (a) static and (b) dynamic conditions.

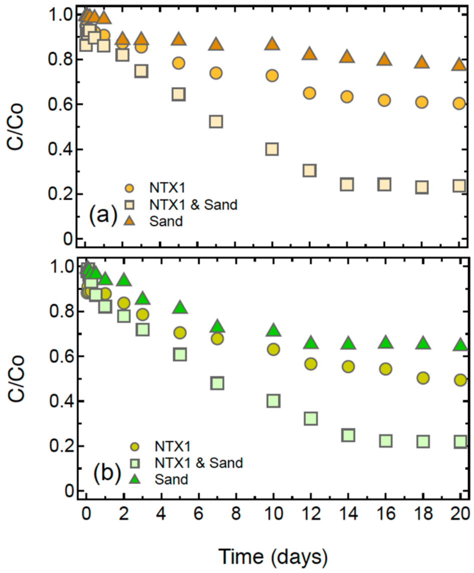

Figure 4. Normalized FA−(2,4-DNPH) concentration values at preselected times under (a) dynamic and (b) static conditions.

Table 2. FA−(2,4-DNPH) Removal after 20 Days Contact Time (%)

adsorbent	static experiments	dynamic experiments	removal increase due to agitation (%)
NTX1	39.6	50.6	28
NTX1 and sand	76.7	78.1	1.8
quartz sand	23.0	35.6	55

removal efficiency than quartz sand. It is worth noting that the mass of nanotubes (20 mg) used was considerably smaller than the quartz sand (14 g). However, pristine multiwalled carbon nanotubes, even in such small quantities, resulted in greater FA−(2,4-DNPH) removal than the quartz sand.

For both static and dynamic conditions, the observed adsorption capacity values (Figure 1) and removal values (Figure 3) followed a similar upward trend. However, in all cases examined, higher FA−(2,4-DNPH) removal was achieved under dynamic conditions, because agitation enhanced the adsorption process, due to increased mass transfer rate and enhanced contact between FA−(2,4-DNPH) molecules and adsorbent surfaces (i.e., suppression of the diffused boundary layer). As shown in Table 2, agitation considerably affected the effectiveness of the adsorbents NTX1 and quartz sand, as the removal values increased by 28% and 55%, respectively. In contrast, when quartz sand was combined with NTX1, no remarkable difference in FA−(2,4-DNPH) removal was observed in the presence of agitation. This was attributed to an apparent balance between the enhanced FA−(2,4-DNPH) removal caused by the increased number of accessible sites and the reduced FA−(2,4-DNPH) removal caused by the decreased secondary porosity due to breakup of the NTX1 aggregates.

It is evident from Figure 4 that the FA−(2,4-DNPH) concentration in the aqueous phase exhibited a continuous downward trend with increasing time. Furthermore, the fitted values of parameters k_{p2} and $C_{eq}^{*}$of the pseudo-second-order kinetic model (see Table 1) ascertained that the quartz sand exhibited lower adsorption capacity values and higher adsorption rates than MWCNTs. FA−(2,4-DNPH) was slowly adsorbed onto the structure of carbon nanotubes. Note that for the interaction between FA−(2,4-DNPH) and quartz sand (Figures 1c,f and 3) adsorption equilibrium was slowly achieved after 10 days of contact time. However, in the presence of MWCNTs, adsorption equilibrium began after 14 days, and in some cases, the experimental duration was not sufficient to achieve equilibrium (see Figure 1c,d).

It is worth noting that potentially available adsorption sites on open-ended single-walled carbon nanotubes bundles (SWCNTs bundles) are (i) periphery grooves formed between adjacent tubes, (ii) external curved surfaces of individual nanotubes of the bundles, (iii) large diameter gaps formed between the bundles (i.e., interstitial channels), and (iv) hollow internal sites.[65] As opposed to SWCNTs, the interaction of MWCNTs, which occurs due to van der Waals forces, does not result in bundle formation but in the entanglement of individual MWCNTs. Thus, in case of open-ended MWCNTs, the adsorption reactive sites probably consisted of pores on the external walls of the nanostructures, aggregated pores between the adhered tubes, and small hollow internal sites of the individual MWCNTs, as well as possible defects formed on MWCNTs surfaces.[93]

However, the MWCNTs used in this study were the closed type (i.e., closed at both ends); thus, adsorption was expected to take place only on external surfaces and on interstitial spaces of the entangled tubes, while voids between coaxial MWCNTs as well as the internal pore surface of individual nanotubes were inaccessible.[94−96]

Initially, the adsorption process of organic compounds onto pristine and closed-ended MWCNTs probably occurred in the largest interstitial spaces of the entangled tubes, and subsequently, absorption occurred on the outer walls of individual nanotubes.[94,97] Therefore, the delay in adsorption equilibrium observed in this study was probably due to the fact that equilibrium was reached more slowly on the aggregated pores of the interstitial spaces formed between the entangled tubes than the external sites of individual MWCNTs.[65] The fact that the experimental results were satisfactorily described by the pseudo-second-order model suggested that chemical sorption probably occurred between FA−(2,4-DNPH) and the two adsorbents examined. However, on the basis of the C_{eq}^{*}fitted values listed in Table 1, FA−(2,4-DNPH) adsorption onto MWCNTs and quartz sand was slow.

It is obvious from Figure 2 that the Weber-Morris plots of the experimental data consisted of three linear parts of different slopes. The slopes of each linear part, the corresponding *y*-intercepts of the lines, as well as the correlation coefficients calculated using linear regression were presented in Table 1. Given that the fitted lines do not pass through the origin ($C \neq 0$), it was revealed that intra-aggregate diffusion was not the only rate-limiting step and that probably film diffusion significantly contributed to the sorption process. In all cases examined, the first linear part of the plots ($0 < t \leq 1$ day) represented the rapid mass transfer of FA−(2,4-DNPH) molecules across the boundary liquid film (positive *y*-axis intercepts). According to Kumar and Gaur,[98] the binding process is usually fast. The second linear part of the plots represented the intraparticle diffusion of FA−(2,4-DNPH) molecules. Note than the observed negative *y*-axis intercepts of the second linear part indicated that probably pore diffusion resistance occurred during the adsorption process. The third linear part, with almost zero gradient, confirmed that an adsorption equilibrium of the system was established. In Figure 2c,d, there existed three linear parts, but no adsorption equilibrium was reached over the experimental period. The third linear part in Figure 2c,d suggested that further FA−(2,4-DNPH) diffusion within MWCNTs occurred after 14 days of contact time.

The weak affinity of FA−(2,4-DNPH) for quartz sand could probably be explained by the low octanol/water distribution coefficient ($\log K_{ow} = 0.35$) of FA. On the basis of the RMSE values determined for the two models (see Table 1), it is evident that the experimental data, with the exception of the case of FA−(2,4-DNPH) interaction with quartz sand under static conditions, were best described by the Weber-Morris intraparticle diffusion model.

5. SUMMARY AND CONCLUSIONS

The experimental results of this study suggested that the binding affinity of FA−(2,4-DNPH) for quartz sand was low, while adsorption was enhanced in the presence of MWCNTs. In addition, FA−(2,4-DNPH) adsorption onto quartz sand and MWCNTs was more pronounced under dynamic than static conditions, probably due to agitation. Also, it was shown, in most of the cases considered, that the adsorption experimental data were better described by the Weber-Morris intraparticle diffusion model than the pseudo-second-order kinetic model. Therefore, initially, a rapid surface chemisorption of FA−(2,4-DNPH) onto available external adsorption sites of sand and MWCNTs (i.e., outer convex nanotube walls) occurred, and subsequently, a slower intra-aggregate (pore) diffusion of FA−(2,4-DNPH) onto interstitial spaces of entangled MWCNTs, through the surface mesopores, probably took place. The observed slow approach to adsorption equilibrium in the case of NTX1 and quartz sand mixed with NTX1 can be attributed to the fact that diffusion was the limiting step.

The findings of this study suggested that FA−(2,4-DNPH) can not be retained by quartz sand. However, a mixture of 14 g of quartz sand and 20 mg of no-functional multiwalled carbon nanotubes can significantly remove FA−(2,4-DNPH) from aqueous samples. Therefore, engineered MWCNTs could be promising adsorbent materials for development of new filtration techniques and for groundwater remediation.

AUTHOR INFORMATION

Corresponding Author

*E-mail: cvc@enveng.tuc.gr.

ORCID

Constantinos V. Chrysikopoulos: 0000-0003-4722-8697

Notes

The authors declare no competing financial interest.

ACKNOWLEDGMENTS

This research did not receive any specific grant from funding agencies in the public, commercial, or not-for-profit sectors. The authors are thankful to R. Sarika and T. Fountouli for valuable laboratory assistance.

REFERENCES

(1) Liteplo, R. G.; Beauchamp, R.; Meek, M. E.; Chénier, R. *Formaldehyde*; Concise International Chemical Assessment Document 40; World Health Organization: Geneva, Switzerland, 2002.

(2) Paliulis, D. Removal of formaldehyde from synthetic wastewater using natural and modified zeolites. *Pol. J. Environ. Stud.* **2016**, *25* (1), 251−257.

(3) Oliveira, S. V.; Moraes, E. M.; Adorno, M. A.; Varesche, M. B.; Foresti, E.; Zaiat, M. Formaldehyde degradation in an anaerobic packed-bed bioreactor. *Water Res.* **2004**, *38*, 1685−1694.

(4) Moussavi, G.; Yazdanbakhsh, A.; Heidarizad, M. The removal of formaldehyde from concentrated synthetic wastewater using O_3/MgO/H_2O_2 process integrated with the biological treatment. *J. Hazard. Mater.* **2009**, *171*, 907−913.

(5) Raja Priya, K.; Sandhya, S.; Swaminathan, K. Kinetic analysis of treatment of formaldehyde containing wastewater in UAFB reactor. *Chem. Eng. J.* **2009**, *148*, 212−216.

(6) Agarwal, M.; Dave, M.; Upadhayaya, S. Adsorption of formaldehyde on treated activated carbon and activated alumina. *Curr. World Environ.* **2011**, *6*, 53−59.

(7) Guimarães, J. R.; Farah, C. R.; Maniero, M. G.; Fadini, P. S. Degradation of formaldehyde by advanced oxidation processes. *J. Environ. Manage.* **2012**, *107*, 96−101.

(8) Moussavi, G.; Bagheri, A.; Khavanin, A. The investigation of degradation and mineralization of high concentrations of formaldehyde in an electro-Fenton process combined with the biodegradation. *J. Hazard. Mater.* **2012**, *237−238*, 147−152.

(9) Lalonde, B. A.; Ernst, W.; Garron, C. Formaldehyde concentration in discharge from land based aquaculture facilities in Atlantic Canada. *Bull. Environ. Contam. Toxicol.* **2015**, *94*, 444−447.

(10) Yasri, N. G.; Seddik, H.; Mosallb, M. A. Spectrophotometric determination of formaldehyde based on the telomerization reaction of tryptamine. *Arabian J. Chem.* **2015**, *8*, 487−494.

(11) Lu, Z.; Hegemann, W. Anaerobic toxicity and biodegradation of formaldehyde in batch cultures. *Water Res.* **1998**, *32*, 209−215.

(12) Hohreiter, D. W.; Rigg, D. K. Derivation of ambient water quality criteria for formaldehyde. *Chemosphere* **2001**, *45*, 471−486.

(13) Regulation (EC) No 1271/2008 of the European Parliament and of the Council of the 16 December 2008 on classification, labeling and packaging of substances and mixtures, amending and repealing Directives 67/548/EEC and 1999/45/EC, and amending Regulation (EC) No 1907/2006. *Official Journal of European Union*; L353/1 31/12/2008; 2008.

(14) International Agency for Research on Cancer (IARC). Chemical agents and related occupations: a review of human carcinogens. In *IARC Monographs on the Evaluation of Carcinogenic Risks to Humans*; World Health Organization (WHO): Geneva, Switzerland, 2012; Vol. *100F*; pp 401−430.

(15) Hill, A. A.; Lipert, R. J.; Fritz, J. S.; Porter, M. D. A rapid, simple method for determining formaldehyde in drinking water using colorimetric-solid phase extraction. *Talanta* **2009**, *77*, 1405−1408.

(16) Tang, X.; Bai, Y.; Duong, A.; Smith, M. T.; Li, L.; Zhang, L. Formaldehyde in China: Production, consumption, exposure levels, and health effects. *Environ. Int.* **2009**, *35*, 1210−1224.

(17) Soman, A.; Qiu, Y.; Chan, L. Q. HPLC-UV method development and validation for the determination of low level formaldehyde in a drug substance. *J. Chromatogr. Sci.* **2008**, *46*, 461−465.

(18) Rivero, R. T.; Topiwala, V. Quantitative determination of formaldehyde in cosmetics using a combined solid-phase microextraction-isotope dilution mass spectrometry method. *J. Chromatogr. A* **2004**, *1029*, 217−222.

(19) Kenessov, B.; Sailaukhanuly, Ү.; Koziel, J. A.; Carlsen, L.; Nauryzbayev, M. GC-MS and GC-NPD determination of formaldehyde dimethylhydrazone in water using SPME. *Chromatographia* **2011**, *73*, 123−128.

(20) Shin, H.; Lim, H. Simple determination of formaldehyde in fermented foods by HS-SPME/GC-MS. *Int. J. Food Sci. Technol.* **2012**, *47*, 350−356.

(21) de Souza, A.; Cunha, I. C. M.; Chagas, J. O.; Pontes Carlos, E. B.; Santos, L. L.; Campos e Figueredo, T. R.; Machado, L. A. L.; Osório, V. M.; Vieira, K. M.; Lobo, F. A. Use of mass spectrometry for the determination of formaldehyde in samples potentially toxic to humans: a brief review. In *Mass Spectrometry* [Online]; Aliofkhazraei, M., Ed.; INTECH: London, 2017; Chapter 9; https://cdn.intechopen.com/pdfs/55396.pdf (accessed August 10, 2018).

(22) Jones, S. B.; Terry, C. M.; Lister, T. E.; Johnson, D. C. Determination of submicromolar concentrations of formaldehyde by liquid chromatography. *Anal. Chem.* **1999**, *71*, 4030−4033.

(23) Tsai, C. F.; Shiau, H. W.; Lee, S. C.; Chou, S. S. Determination of low-molecule-weight aldehydes in packed drinking water by high performance liquid chromatography. *J. Food Drug Anal.* **2003**, *11*, 46−52.

(24) Peng, B.; Zhang, J.; Wu, C.; Li, S.; Li, Y.; Gao, H.; Lu, R.; Zhou, W. Use of ionic liquid-based dispersive liquid-liquid microextraction and high-performance liquid chromatography to detect formaldehyde in air, water and soil samples. *J. Liq. Chromatogr. Relat. Technol.* **2014**, *37*, 815−828.

(25) U.S. Environmental Protection Agency (USEPA). *Method 1667, Revision A: Formaldehyde, isobutyraldehyde, and furfural by derivatization followed by high performance liquid chromatography*; Office of Water, U.S. Environmental Protection Agency: Washington, DC, 1998; https://www.epa.gov/sites/production/files/2015-09/documents/method_1667a_1998.pdf (accessed August 10, 2018).

(26) U.S. Environmental Protection Agency (USEPA). *Method 8315A (SW-846): Determination of carbonyl compounds by high performance liquid chromatography (HPLC)*, Revision 1; USEPA: Washington, DC, 1996; https://www.epa.gov/sites/production/files/2015-07/documents/epa-8315a.pdf (accessed August 10, 2018).

(27) Eichelberger, J. W.; Bashe, W. J. *Method 554, Determination of carbonyl compounds in drinking water by DNPH derivatization and high performance liquid chromatography (HPLC)*, Revision 1.0; Environmental Monitoring Systems Laboratory; Office of Research and Development; U.S. Environmental Protection Agency: Cincinnati, Ohio, 1992.

(28) United States Department of Health and Human Services (HHS); Centers for Disease Control and Prevention; National Institute for Occupational Safety and Health. *NIOSH Pocket Guide to Chemical Hazards*, 3rd ed.; DHHS (NIOSH) Publication No. 2005-149; U.S. Government Printing Office: Washington, DC, 2007; https://www.cdc.gov/niosh/docs/2005-149/pdfs/2005-149.pdf (accessed August 10, 2018).

(29) U.S. Environmental Protection Agency (USEPA). *Standards Applicable to Generators of Hazardous Waste*; Title 40-Protection of Environment; Vol. 27; Part 262; U.S. Government Printing Office: Washington, DC, 2012.

(30) U.S. Environmental Protection Agency (USEPA). *Profile and management options for EPA laboratory generated mixed waste (Final Report)*; EPA 402-R-96-015; Center for Remediation Technology and Tools, Radiation Protection Division, Office of Radiation and Indoor Air, U.S. Environmental Protection Agency: Washington, DC, 1996.

(31) Saravanan, R.; Khan, M. M.; Gupta, V. K.; Mosquera, E.; Gracia, F.; Narayanan, V.; Stephen, A. ZnO/Ag/CdO nanocomposite for visible light-induced photocatalytic degradation of industrial textile effluents. *J. Colloid Interface Sci.* **2015**, *452*, 126−133.

(32) Karthikeyan, S.; Gupta, V. K.; Boopathy, R.; Titus, A.; Sekaran, G. A new approach for the degradation of high concentration of aromatic amine by heterocatalytic Fenton oxidation: Kinetic and spectroscopic studies. *J. Mol. Liq.* **2012**, *173*, 153−163.

(33) Saravanan, R.; Sacari, E.; Gracia, F.; Khan, M. M.; Mosquera, E.; Gupta, V. K. Conducting PANI stimulated ZnO system for visible light photocatalytic degradation of coloured dyes. *J. Mol. Liq.* **2016**, *221*, 1029−1033.

(34) Gupta, V. K.; Jain, R.; Nayak, A.; Agarwal, S.; Shrivastava, M. Removal of the hazardous dye-Tartrazine by photodegradation on titanium dioxide surface. *Mater. Sci. Eng., C* **2011**, *31*, 1062−1067.

(35) Saravanan, R.; Karthikeyan, S.; Gupta, V. K.; Sekaran, G.; Narayanan, V.; Stephen, A. Enhanced photocatalytic activity of ZnO/CuO nanocomposite for the degradation of textile dye on visible light illumination. *Mater. Sci. Eng., C* **2013**, *33*, 91−98.

(36) Saravanan, R.; Karthikeyan, N.; Gupta, V. K.; Thirumal, E.; Thangadurai, P.; Narayanan, V.; Stephen, A. ZnO/Ag nanocomposite: An efficient catalyst for degradation studies of textile effluents under visible light. *Mater. Sci. Eng., C* **2013**, *33*, 2235−2244.

(37) Rajendran, S.; Khan, M. M.; Gracia, F.; Qin, J.; Gupta, V. K.; Arumainathan, S. Ce^{3+}-ion-induced visible-light photocatalytic degradation and electrochemical activity of ZnO/CeO_2 nanocomposite. *Sci. Rep.* **2016**, *6*, 3164.

(38) Ahmaruzzaman, M.; Gupta, V. K. Rice husk and its ash as low-cost adsorbents in water and wastewater treatment. *Ind. Eng. Chem. Res.* **2011**, *50*, 13589−13613.

(39) Gupta, V. K.; Nayak, A.; Agarwal, S. Bioadsorbents for remediation of heavy metals: Current status and their future prospects. *Environ. Eng. Res.* **2015**, *20* (1), 1−18.

(40) Gupta, V. K.; Nayak, A.; Agarwal, S.; Tyagi, I. Potential of activated carbon from waste rubber tire for the adsorption of phenolics: Effect of pre-treatment conditions. *J. Colloid Interface Sci.* **2014**, *417*, 420−430.

(41) Gupta, V. K.; Saleh, T. A. Sorption of pollutants by porous carbon, carbon nanotubes and fullerene - An overview. *Environ. Sci. Pollut. Res.* **2013**, *20*, 2828−2843.

(42) Gupta, V. K.; Kumar, R.; Nayak, A.; Saleh, T. A.; Barakat, M. A. Adsorptive removal of dyes from aqueous solution onto carbon nanotubes: A review. *Adv. Colloid Interface Sci.* **2013**, *193−194*, 24−43.

(43) Robati, D.; Mirza, B.; Rajabi, M.; Moradi, O.; Tyagi, I.; Agarwal, S.; Gupta, V. K. Removal of hazardous dyes-BR 12 and methyl orange using graphene oxide as an adsorbent from aqueous phase. *Chem. Eng. J.* **2016**, *284*, 687−697.

(44) Aqel, A.; El-Nour, K. M. M. A.; Ammar, R. A. A.; Al-Warthan, A. Carbon nanotubes, science and technology part (I) structure, synthesis and characterization. *Arabian J. Chem.* **2012**, *5*, 1−23.

(45) Rashad, A. A.; Noaman, R.; Mohammed, S. A.; Yousif, E. Synthesis of carbon nanotube: a review. *J. Nanosci. Technol.* **2016**, *2*, 155−162.

(46) Deb, A. K.; Chusuei, C. C. Aqueous solution surface chemistry of carbon nanotubes. In *Physical and Chemical Properties of Carbon Nanotubes* [Online], 1st ed.; Suzuki, S., Ed.; INTECH: Croatia, 2013; ISBN 978-953-51-1002-6.

(47) Yuca, N.; Karatepe, N.; Yakuphanoğlu, F.; Gürsel, Y. H. Thermal and electrical properties of carbon nanotube based materials. *Acta Phys. Pol., A* **2013**, *123*, 352−354.

(48) Chu, K.; Kim, D.; Sohn, Y.; Lee, S.; Moon, C.; Park, S. Electrical and thermal properties of carbon-nanotube composite for

flexible electric heating-unit applications. *IEEE Electron Device Lett.* **2013**, *34*, 668−670.

(49) Avouris, P.; Chen, J. Nanotube electronics and optoelectronics. *Mater. Today* **2006**, *9*, 46−54.

(50) Avouris, P.; Freitag, M.; Perebeinos, V. Carbon-nanotube photonics and optoelectronics. *Nat. Photonics* **2008**, *2*, 341−350.

(51) Otte, K. G. A study of the thermal properties of commercially available multi-walled carbon nanotubes and gold nanowires. MS Thesis, Vanderbilt University, Nashville, TN, 2013.

(52) Spitalsky, Z.; Tasis, D.; Papagelis, K.; Galiotis, C. Carbon nanotube-polymer composites: chemistry, processing, mechanical and electrical properties. *Prog. Polym. Sci.* **2010**, *35*, 357−401.

(53) Kuan, C.-F.; Kuan, H.-C.; Ma, C-C. M.; Chen, C.-H. Mechanical and electrical properties of multi-wall carbon nanotube/poly(lactic acid) composites. *J. Phys. Chem. Solids* **2008**, *69*, 1395−1398.

(54) Coleman, J. N.; Khan, U.; Blau, W. J.; Gun'ko, Y. K. Small but strong: a review of the mechanical properties of carbon nanotube-polymer composites. *Carbon* **2006**, *44*, 1624−1652.

(55) Ruoff, R. S.; Qian, D.; Liu, W. K. Mechanical properties of carbon nanotubes: theoretical predictions and experimental measurements. *C. R. Phys.* **2003**, *4*, 993−1008.

(56) Notarianni, M.; Liu, J.; Vernon, K.; Motta, N. Synthesis and applications of carbon nanomaterials for energy generation and storage. *Beilstein J. Nanotechnol.* **2016**, *7*, 149−196.

(57) Baughman, R. H.; Zakhidov, A. A.; de Heer, W. A. Carbon nanotubes-the route toward applications. *Science* **2002**, *297*, 787−792.

(58) Stoner, B. R.; Brown, B.; Glass, J. T. Selected topics on the synthesis, properties and applications of multiwalled carbon nanotubes. *Diamond Relat. Mater.* **2014**, *42*, 49−57.

(59) Geetha, P.; Lakshmi, N. V.; Parimalasundar, E. Carbon nanotube field effect transistor: A review. *Int. J. Sci. Res. Develop.* **2017**, *5*, 243−252.

(60) Bianco, A.; Kostarelos, K.; Prato, M. Applications of carbon nanotubes in drug delivery. *Curr. Opin. Chem. Biol.* **2005**, *9*, 674−679.

(61) Mahmood, M.; Karmakar, A.; Fejleh, A.; Mocan, T.; Iancu, C.; Mocan, L.; Iancu, D. T.; Xu, Y.; Dervishi, E.; Li, Z.; Biris, A. R.; Agarwal, R.; Ali, N.; Galanzha, E. I.; Biris, A. S.; Zharov, V. P. Synergistic enhancement of cancer therapy using a combination of carbon nanotubes and anti-tumor drug. *Nanomedicine* **2009**, *4*, 883−893.

(62) Kamalha, E.; Shi, X.; Mwasiagi, J. I.; Zeng, Y. Nanotechnology and carbon nanotubes; A review of potential in drug delivery. *Macromol. Res.* **2012**, *20*, 891−898.

(63) Tan, J. M.; Arulselvan, P.; Fakurazi, S.; Ithnin, H.; Hussein, M. Z. A review on characterizations and biocompatibility of functionalized carbon nanotubes in drug delivery design. *J. Nanomater.* **2014**, *2014*, 917024.

(64) Pan, B.; Xing, B. Adsorption mechanisms of organic chemicals on carbon nanotubes. *Environ. Sci. Technol.* **2008**, *42*, 9005−9013.

(65) Ren, X.; Chen, C.; Nagatsu, M.; Wang, X. Carbon nanotubes as adsorbents in environmental pollution management: A review. *Chem. Eng. J.* **2011**, *170*, 395−410.

(66) Mauter, M. S.; Elimelech, M. Environmental applications of carbon-based nanomaterials. *Environ. Sci. Technol.* **2008**, *42*, 5843−5859.

(67) Ong, Y. T.; Ahmad, A. L.; Zein, S. H. S.; Tan, S. H. A review on carbon nanotubes in an environmental protection and green engineering perspective. *Braz. J. Chem. Eng.* **2010**, *27*, 227−242.

(68) Tan, C. W.; Tan, K. H.; Ong, Y. T.; Mohamed, A. R.; Zein, S. H. S.; Tan, S. H. Energy and environmental applications of carbon nanotubes. *Environ. Chem. Lett.* **2012**, *10*, 265−273.

(69) Yang, K.; Zhu, L.; Xing, B. Adsorption of polycyclic aromatic hydrocarbons by carbon nanomaterials. *Environ. Sci. Technol.* **2006**, *40*, 1855−1861.

(70) Long, R. Q.; Yang, R. T. Carbon nanotubes as superior sorbent for dioxin removal. *J. Am. Chem. Soc.* **2001**, *123*, 2058−2059.

(71) Li, Y. H.; Wang, S.; Zhang, X.; Wei, J.; Xu, C.; Luan, Z.; Wu, D. Adsorption of fluoride from water by aligned carbon nanotubes. *Mater. Res. Bull.* **2003**, *38*, 469−476.

(72) Chen, Z.; Zhang, L.; Tang, Y.; Jia, Z. Adsorption of nicotine and tar from the mainstream smoke of cigarettes by oxidized carbon nanotubes. *Appl. Surf. Sci.* **2006**, *252*, 2933−2937.

(73) Lu, C.; Chung, Y. L.; Chang, K. F. Adsorption of trihalomethanes from water with carbon nanotubes. *Water Res.* **2005**, *39*, 1183−1189.

(74) Ji, L.; Chen, W.; Duan, L.; Zhu, D. Mechanisms for strong adsorption of tetracycline to carbon nanotubes: a comparative study using activated carbon and graphite as adsorbents. *Environ. Sci. Technol.* **2009**, *43*, 2322−2327.

(75) Ji, L.; Chen, W.; Zheng, S.; Xu, Z.; Zhu, D. Adsorption of sulfonamide antibiotics to multiwalled carbon nanotubes. *Langmuir* **2009**, *25*, 11608−11613.

(76) Machado, F. M.; Bergmann, C. P.; Lima, E. C.; Adebayo, M. A.; Fagan, S. B. Adsorption of a textile dye from aqueous solutions by carbon nanotubes. *Mater. Res.* **2014**, *17*, 153−160.

(77) Saleh, T. A.; Gupta, V. K. Photo-catalyzed degradation of hazardous dye methyl orange by use of a composite catalyst consisting of multi-walled carbon nanotubes and titanium dioxide. *J. Colloid Interface Sci.* **2012**, *371*, 101−106.

(78) Black, C. A., Ed. *Method of soil analysis, Part 2, Chemical and microbiological properties*; American Society of Agronomy, Inc.; Madison: Wisconsin USA, 1965.

(79) Syngouna, V. I.; Chrysikopoulos, C. V. Transport of biocolloids in water saturated columns packed with sand: Effect of grain size and pore water velocity. *J. Contam. Hydrol.* **2012**, *129−130*, 11−24.

(80) Jensen, K. A.; Bøgelund, J.; Jackson, P.; Jacobsen, N. R.; Birkedal, R.; Clausen, P. A.; Saber, A. T.; Wallin, H.; Vogel, U. B. *Appendices: Carbon nanotubes*; Appendices for environmental project No. 1805; Ministry of Environment and Food of Denmark; Danish Environmental Protection Agency: Copenhagen, Denmark, 2015; https://www2.mst.dk/Udgiv/publications/2015/12/978-87-93352-98-8_appendices.pdf (accessed August 10, 2018).

(81) Qiu, H.; Lv, L.; Pan, B.; Zhang, Q.; Zhang, W.; Zhang, Q. Critical review in adsorption kinetic models. *J. Zhejiang Univ., Sci., A* **2009**, *10*, 716−724.

(82) Sotirelis, N. P.; Chrysikopoulos, C. V. Interaction between graphene oxide nanoparticles and quartz sand. *Environ. Sci. Technol.* **2015**, *49*, 13413−13421.

(83) Weber, W. J.; Morris, J. C. Kinetics of adsorption on carbon from solutions. *J. Sanit. Eng. Div.* **1963**, *89*, 31−60.

(84) Srihari, V.; Babu, S. M.; Das, A. Kinetics of phenol sorption by raw agrowastes. *J. Appl. Sci.* **2006**, *6*, 47−50.

(85) Itodo, A. U.; Abdulrahman, F. W.; Hassan, L. G.; Maigandi, S. A.; Itodo, H. U. Intraparticle diffusion and intraparticulate diffusivities of herbicide on derived activated carbon. *Researcher* **2010**, *2*, 74−86.

(86) McKay, G.; Poots, V. J. P. Kinetics and diffusion processes in colour removal from effluents using wood as adsorbents. *J. Chem. Technol. Biotechnol.* **1980**, *30*, 279−292.

(87) McKay, G. The adsorption of dyestuffs from aqueous solutions using activated carbon. iii Intraparticle diffusion processes. *J. Chem. Technol. Biotechnol., Chem. Technol.* **1983**, *33* (A), 196−204.

(88) Wu, F. C.; Tseng, R. L.; Juang, R. S. Initial behavior of intraparticle diffusion model used in the description of adsorption kinetics. *Chem. Eng. J.* **2009**, *153*, 1−8.

(89) Pontius, R.; Thontteh, O.; Chen, H. Components of information for multiple resolution comparison between maps that share a real variable. *Environ. Ecol. Stat.* **2008**, *15*, 111−142.

(90) Willmott, C.; Matsuura, K. On the use of dimensioned measures of error to evaluate the performance of spatial interpolators. *Int. J. Geogr. Inf. Sci.* **2006**, *20*, 89−102.

(91) Katzourakis, V. E.; Chrysikopoulos, C. V. Fitting the transport and attachment of dense biocolloids in one-dimensional porous media: ColloidFit. *Groundwater* **2017**, *55*, 156−159.

(92) Sim, Y.; Chrysikopoulos, C. V. Analytical models for one-dimensional virus transport in saturated porous media. *Water Resour. Res.* **1995**, *31*, 1429−1437.

(93) Machado, F. M.; Fagan, S. B.; da Silva, I. Z.; de Andrade, M. J. Carbon Nanoadsorbents. In *Carbon Nanomaterials as Adsorbents for Environmental and Biological Applications, Carbon Nanostructure*, 1st ed.; Bergmann, C. P., Machado, F. M., Eds.; Springer International Publishing: New York City, 2015; pp 11−32.

(94) Babaa, M. R.; Dupont-Pavlovsky, N.; McRae, E.; Masenelli-Varlot, K. Physical adsorption of carbon tetrachloride on as-produced and on mechanically opened single walled carbon nanotubes. *Carbon* **2004**, *42*, 1549−1554.

(95) Bienfait, M.; Zeppenfeld, P.; Dupont-Pavlovsky, N.; Muris, M.; Johnson, M. R.; Wilson, T.; DePies, M.; Vilches, O. E. Thermodynamics and structure of hydrogen, methane, argon, oxygen, and carbon dioxide adsorbed on single-wall carbon nanotube bundles. *Phys. Rev. B: Condens. Matter Mater. Phys.* **2004**, *70*, No. 035410.

(96) Heroux, L.; Krungleviciute, V.; Calbi, M. M.; Migone, A. D. CF_4 on carbon nanotubes: physisorption on grooves and external surfaces. *J. Phys. Chem. B* **2006**, *110*, 12597−12602.

(97) Muris, M.; Dupont-Pavlovsky, N.; Bienfait, M.; Zeppenfeld, P. Where are the molecules adsorbed on single-walled nanotubes? *Surf. Sci.* **2001**, *492*, 67−74.

(98) Kumar, D.; Gaur, J. P. Chemical reaction-and particle diffusion-based kinetic modeling of metal biosorption by Phormidium sp. -dominated cyanobacterial mat. *Bioresour. Technol.* **2011**, *102*, 633−640.